

## Supporting Information

# Optical Grade Transformation of Monolayer Transition Metal Dichalcogenides via Encapsulation Annealing

Huije Ryu,<sup>‡a</sup> Seong Chul Hong,<sup>‡a</sup> Kangwon Kim,<sup>b</sup> Yeonjoon Jung,<sup>a</sup> Yangjin Lee,<sup>c,d</sup> Kihyun Lee,<sup>c,d</sup>  
Youngbum Kim,<sup>e</sup> Hyunjun Kim,<sup>a</sup> Kenji Watanabe,<sup>f</sup> Takashi Taniguchi,<sup>g</sup> Jeongyong Kim,<sup>e</sup>  
Kwanpyo Kim,<sup>c,d</sup> Hyeonsik Cheong<sup>b</sup> and Gwan-Hyoung Lee<sup>\*a</sup>

<sup>a</sup> Department of Materials Science and Engineering, Seoul National University, Seoul 08826,  
Republic of Korea

<sup>b</sup> Department of Physics, Sogang University, Seoul 04107, Republic of Korea

<sup>c</sup> Department of Physics, Yonsei University, Seoul 03722, Republic of Korea

<sup>d</sup> Center for Nanomedicine, Institute for Basic Science, Seoul, 03722, Republic of Korea

<sup>e</sup> Department of Energy Science, Sungkyunkwan University, Suwon 16419, Republic of Korea

<sup>f</sup> Research Center for Electronic and Optical Materials, National Institute for Materials Science, 1-1  
1 Namiki, Tsukuba 305-0044, Japan

<sup>g</sup> Research Center for Materials Nanoarchitectonics, National Institute for Materials Science, 1-1  
Namiki, Tsukuba 305-0044, Japan

## Defect density calculation

	Total Se atomic positions ( $N_{pse}$ )	Expected Se atom number ( $2 * N_{pse}$ )	Total $V_{Se}$	Total $V_{Se2}$	Defect density (%) $\frac{V_{Se} + 2 \times V_{Se2}}{2 \times N_{pse}}$
As-stacked	62605	125210	409	2	0.33
Annealed	69257	138514	1901	3	1.38

By utilizing ResUNet deep learning model, we extracted the total atomic positions of Selenium, expected Selenium atom number, total selenium vacancies, total diselenium vacancies. Through the extracted data the defect density was calculated using the following equation.

$$\text{Defect density (\%)} = \left( \frac{V_{Se} + 2 \times V_{Se2}}{2 \times N_{pse}} \right)$$

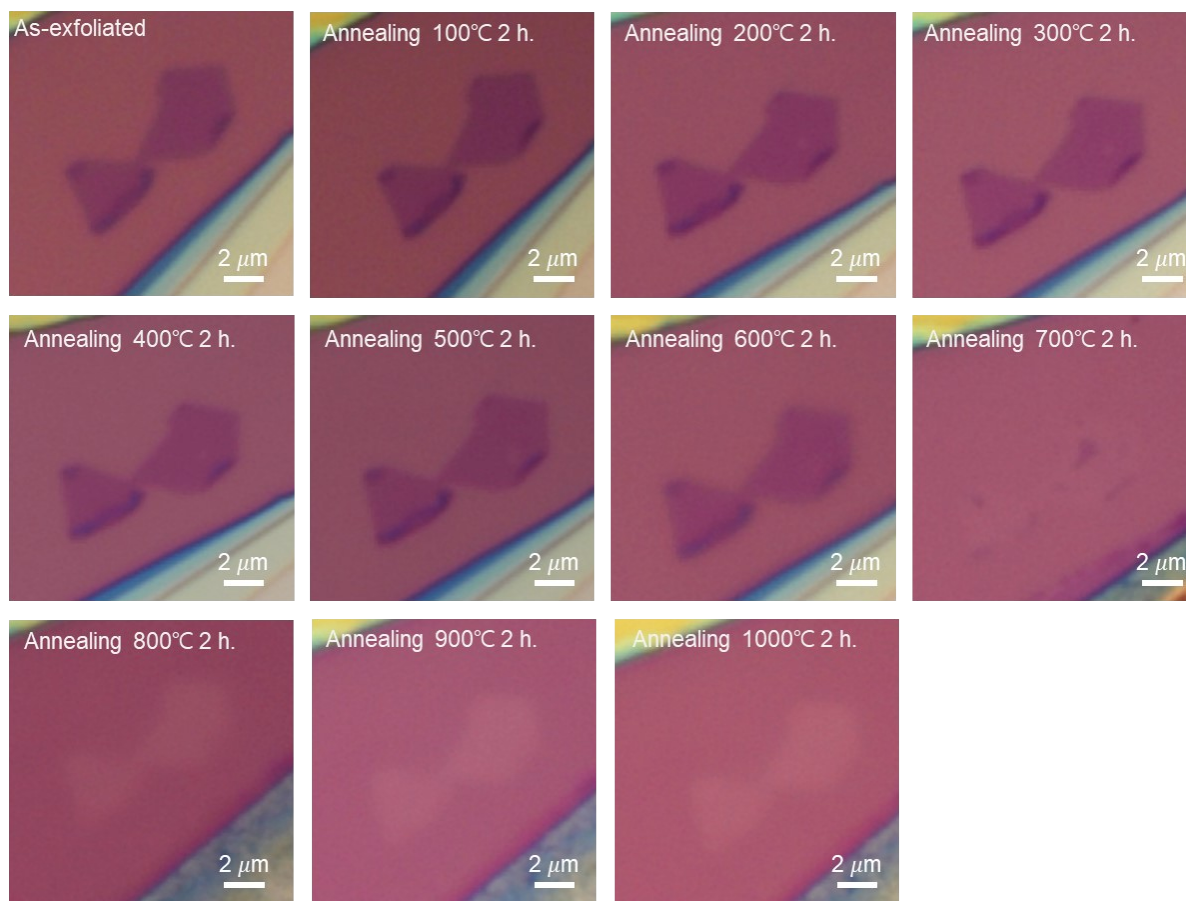


**Figure S1.** Optical microscopic images of exfoliated 1L-WSe<sub>2</sub> before and after annealing at 100-1000°C for 2h. In contrast to hBN-encapsulated 1L-WSe<sub>2</sub>, there was a significant difference in the exfoliated 1L-WSe<sub>2</sub> indicating thermal decomposition.

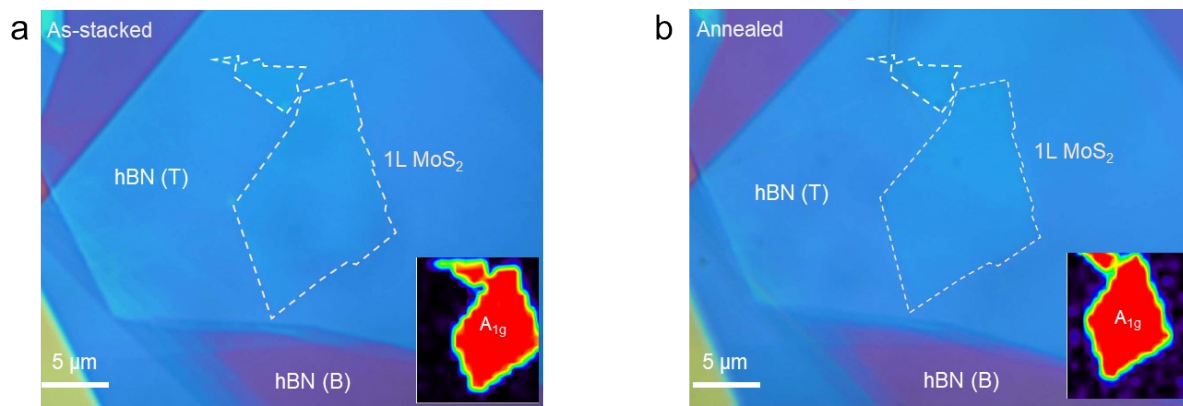


**Figure S2.** Optical microscopic images of hBN-encapsulated 1L-MoS<sub>2</sub> (a) before and (b) after annealing at 900°C for 3 h. Inset Raman peak intensity maps for the A<sub>1g</sub> mode of MoS<sub>2</sub>.

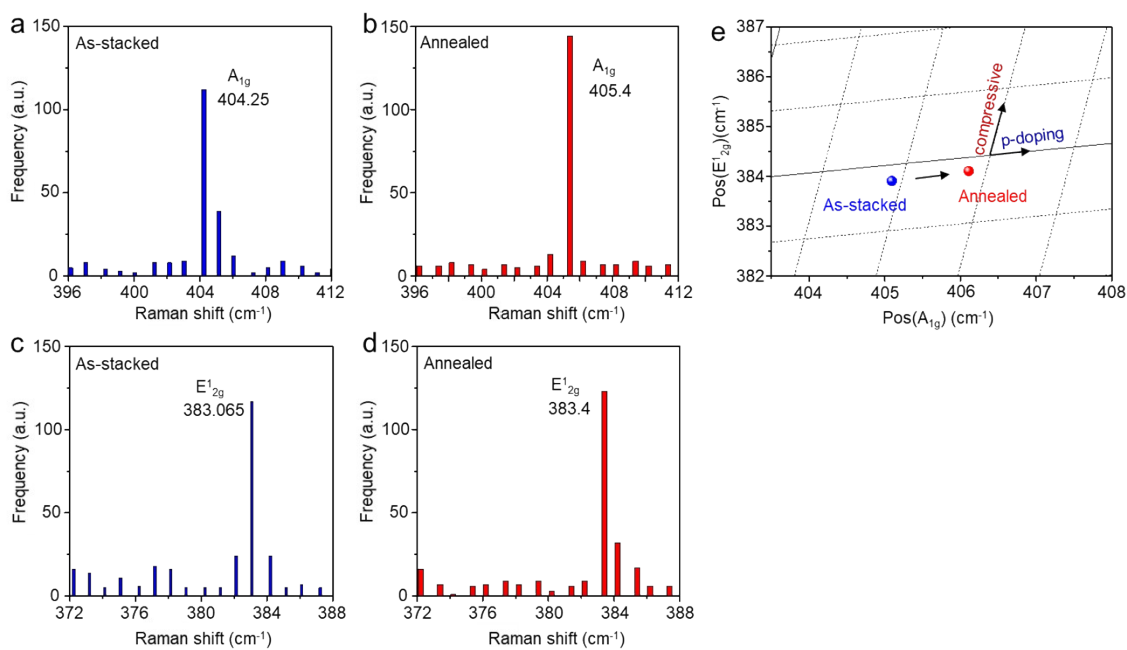


**Figure S3.** Raman peak shift of hBN-encapsulated 1L-MoS<sub>2</sub> before and after annealing. Histogram of (a,b) A<sub>1g</sub> peak position, (c,d) E<sub>12g</sub> peak position of MoS<sub>2</sub> before and after annealing at 900°C for 3 h. (e) A<sub>1g</sub> and E<sub>12g</sub> peak position plots for hBN-encapsulated 1L-MoS<sub>2</sub> before and after encapsulation annealing. A<sub>1g</sub> peak and E<sub>12g</sub> peak position was plotted based on the peak position with the highest frequency in the histogram. The shift in the peak position indicates that the MoS<sub>2</sub> is dedoped by encapsulation annealing.

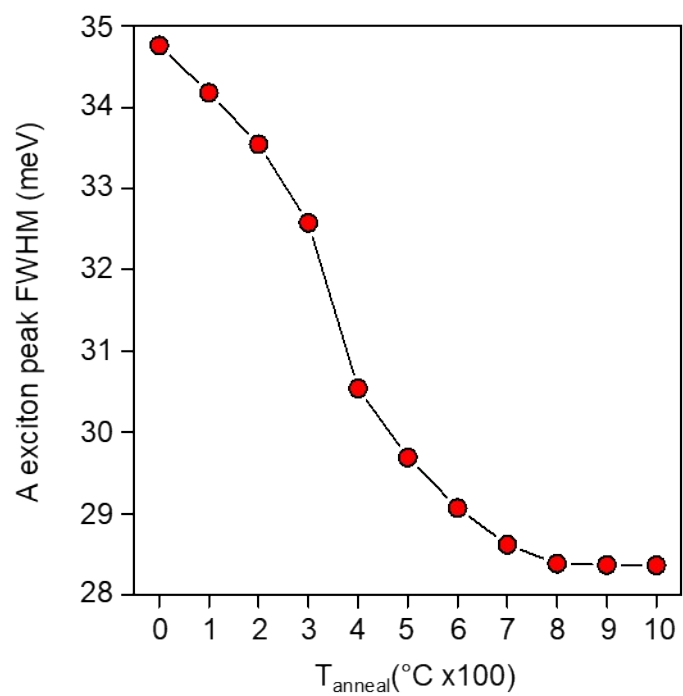


**Figure S4.** Annealing temperature dependent A exciton peak FWHM of hBN-encapsulated 1L-WSe<sub>2</sub>. The FWHM decreases as the annealing temperature increases until 800°C.

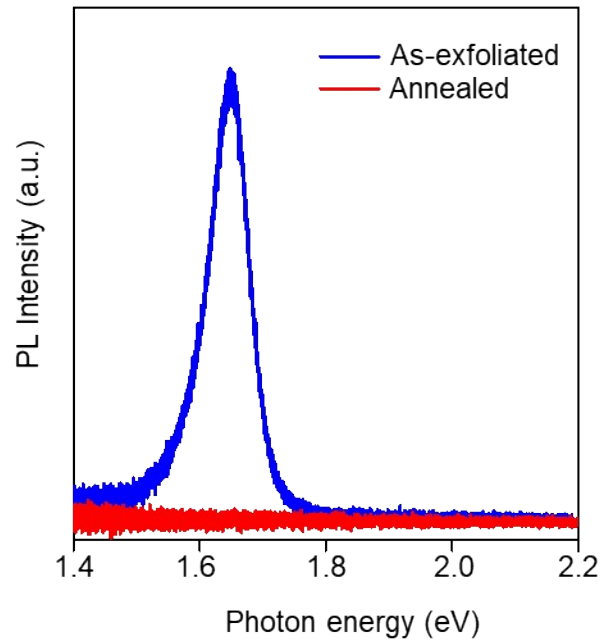


**Figure S5.** PL Intensity spectra of as-exfoliated 1L-WSe<sub>2</sub> before and after annealing at 1000°C for 2h. The PL was quenched after annealing which indicates thermal decomposition of the 1L-WSe<sub>2</sub>.

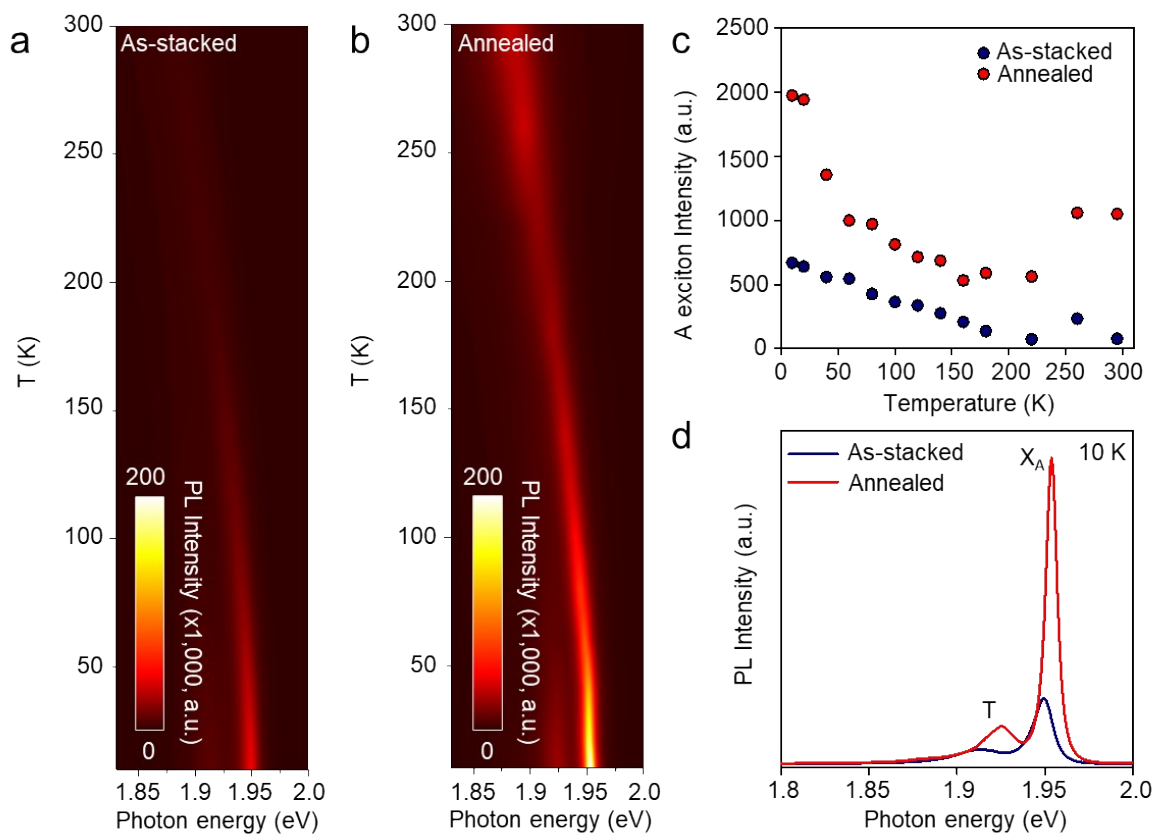


**Figure S6.** Contour plots of PL spectra of 1L-MoS<sub>2</sub> as a function of temperature (from 10 to 300K) (a) before and (b) after annealing. (c) A exciton intensity as a function of temperature of hBN-encapsulated 1L-MoS<sub>2</sub> before (blue) and after annealing (red). (d) PL spectra (10K) of hBN-encapsulated 1L-MoS<sub>2</sub> before (blue) and after annealing (red). The PL intensity of the 1L-MoS<sub>2</sub> increases as the temperature decreases due dominant population of bright excitons at low temperature. The PL intensity of the annealed 1L-MoS<sub>2</sub> was higher than that of as-stacked 1L-MoS<sub>2</sub> across the entire temperature range from 10 to 300K.



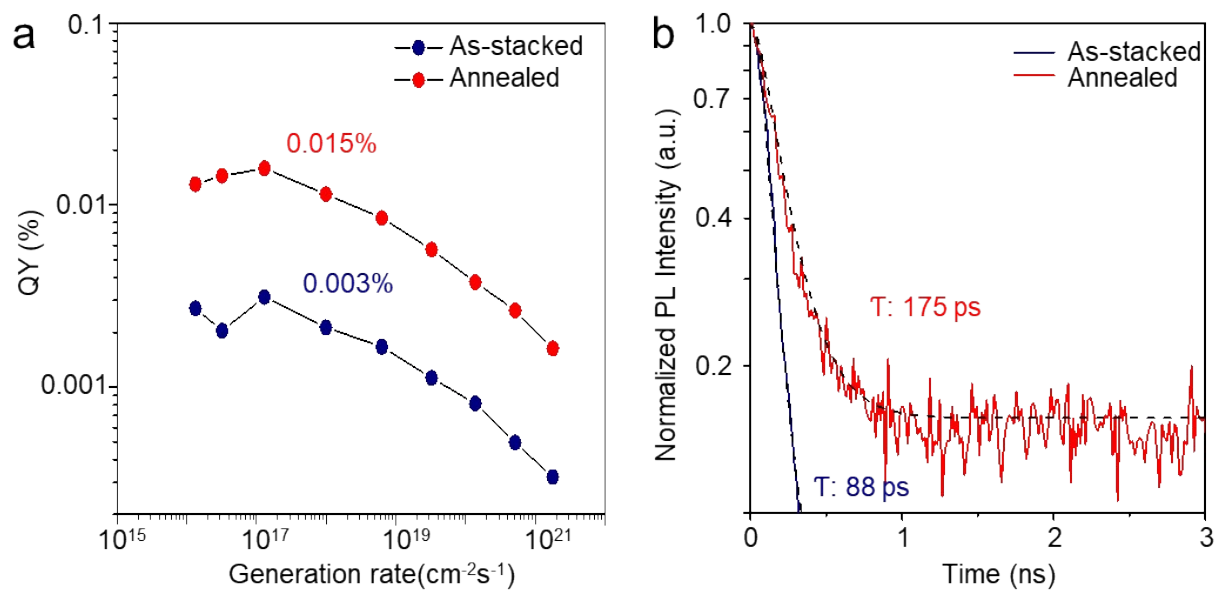


**Figure S7.** (a) Plot of PL QYs as a function of the generation rate and (b) normalized TRPL decay curves for hBN-encapsulated 1L-MoS<sub>2</sub> before (blue) and after annealing (red).-